AD-A103 728 MOTOROLA INC SCOTTSDALE AZ GOVERNMENT ELECTRONICS DIV F/G 20/2
DOUBLY ROTATED CUT SAW DEVICES.(U)
AUG 81 D F WILLIAMS, F Y CHO DAAK20-79-C-0275
UNCLASSIFIED DELET-TR-79-0275-3 NL

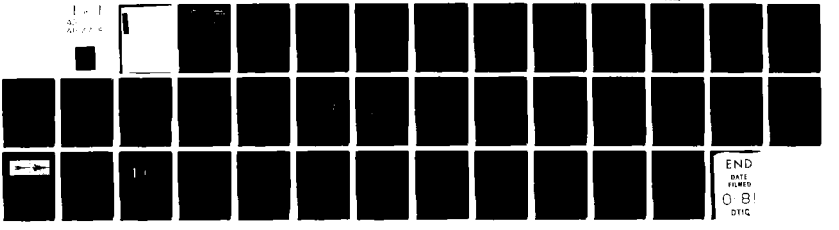

END
DATE FILMED
0 81
DTIC

UNCLASSIFIED

SECURITY CLASSIFICATION OF THIS PAGE (When Data Entered)

REPORT DOCUMENTATION PAGE	READ INSTRUCTIONS BEFORE COMPLETING FORM
1. REPORT NUMBER (18) DELET-TR-79-0275-3	2. GOVT ACCESSION NO.
	3. RECIPIENT'S CATALOG NUMBER no. 3
4. TITLE (and Subtitle) (6) Doubly Rotated Cut SAW Devices	5. TYPE OF REPORT & PERIOD COVERED (9) Interim Report, 1 September 1980 - 1 March 1981
	6. PERFORMING ORG. REPORT NUMBER
7. AUTHOR(s) (10) D.F. Williams, F.Y. Cho	8. CONTRACT OR GRANT NUMBER(s) (15) DAAK20-79-C-0275
9. PERFORMING ORGANIZATION NAME AND ADDRESS Motorola, GED 8201 E. McDowell Rd. Scottsdale, AZ 85252	10. PROGRAM ELEMENT, PROJECT, TASK AREA & WORK UNIT NUMBERS 612705.H94.09.11.01
11. CONTROLLING OFFICE NAME AND ADDRESS (11) Director, US Army Electronics Tech & Devices Lab ATTN: DELET-MM Fort Monmouth, NJ 07703	12. REPORT DATE August 1981
	13. NUMBER OF PAGES 34
14. MONITORING AGENCY NAME & ADDRESS (if different from Controlling Office) 12 37	15. SECURITY CLASS. (of this report) UNCLASSIFIED
	15a. DECLASSIFICATION/DOWNGRADING SCHEDULE

16. DISTRIBUTION STATEMENT (of this Report)

Approved for Public Release; Distribution Unlimited.

17. DISTRIBUTION STATEMENT (of the abstract entered in Block 20, if different from Report)

18. SUPPLEMENTARY NOTES

19. KEY WORDS (Continue on reverse side if necessary and identify by block number)

Surface Acoustic Waves, Quartz, Temperature Coefficient of Frequency, X-Ray Orientation, Power Flow Angle.

20. ABSTRACT (Continue on reverse side if necessary and identify by block number)

The objective of this program is the exploratory development of doubly rotated cuts of quartz possessing superior Surface Acoustic Wave (SAW) properties for applications involving environmentally hardened devices. The key properties examined and optimized both theoretically and experimentally are: first, second and third order Temperature Coefficients of Delay (TCD), piezoelectric coupling factor, power flow angle, Bulk Acoustic Wave (BAW) inverse velocity surfaces, degeneracies and leaky waves, and sensitivities of the above quantities to misorientations and manufacturing tolerances. → next page

DD FORM 1 JAN 79 1473 EDITION OF 1 NOV 65 IS OBSOLETE

UNCLASSIFIED

SECURITY CLASSIFICATION OF THIS PAGE (When Data Entered)

4 of 4

H01077

The program consists of two major task areas comprising an interactive numerical/experimental approach. Task I involves the numerical computation of the key SAW properties for doubly rotated quartz substrates for the purpose of locating promising angular ranges with properties superior to the singly rotated cuts now in existence. More detailed calculations follow to refine the angular coordinates in order to specify cuts for experimental verification in Task II. In Task II, sets of substrates with promising orientations identified in Task I were prepared and SAW device patterns were fabricated for evaluation of the key SAW properties. The experimental results of this task were correlated with the theoretical predictions and an iterative process developed for refinement of both theoretical and experimental parameters. As the program proceeded, working SAW device models were delivered as a demonstration of progress and an indication of the future potential of the doubly rotated cuts. Depending upon the progress made and time and budget limitations, additional properties in the area of nonlinear elasticity will be investigated. This report contains the second iteration of the two major tasks mentioned above; it also contains the discussion on variation of power flow angle as a function of temperature and methods for compensation of the temperature coefficient of frequency as the power flow angle changes.

TABLE OF CONTENTS

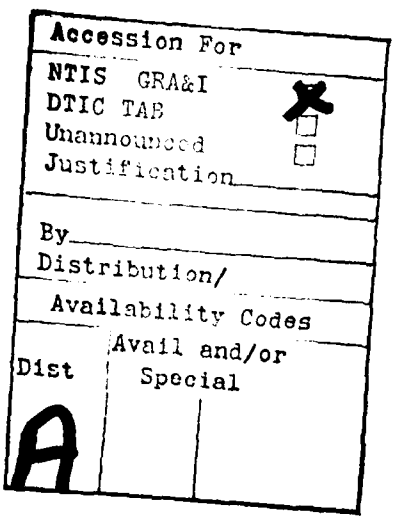

LIST OF ILLUSTRATIONS

SECTION I

INTRODUCTION

1. PROGRAM OBJECTIVE

The objective of this program is the exploratory development of doubly rotated cuts of quartz possessing superior Surface Acoustic Wave (SAW) properties for applications involving environmentally hardened devices. The key properties examined and optimized both theoretically and experimentally are: first, second and third order Temperature Coefficients of Frequency (TCF), piezoelectric coupling factor, power flow angle, Bulk Acoustic Wave (BAW) inverse velocity surfaces, and sensitivities of the above quantities to misorientations and manufacturing tolerances.

2. PROGRAM SCOPE

The program consists of two major task areas comprising an interactive numerical/experimental approach. Task I involves the numerical computation of the key SAW properties for doubly rotated quartz substrates for the purpose of locating angular ranges with properties superior to the singly rotated cuts now in existence. More detailed calculations followed to refine the angular coordinates in order to specify cuts for experimental verification in Task II. In Task II, sets of substrates with promising orientations identified in Task I are prepared and SAW device patterns fabricated for evaluation of the key SAW properties. The experimental results of this task are correlated with the theoretical predictions, and an iterative process develops for refinement of both theoretical and experimental parameters. As the program proceeded, working SAW devices were delivered as a demonstration of progress and an indication of the future potential of the doubly rotated cuts. Depending upon the progress made and time and budget limitations, additional properties in the area of nonlinear elasticity will be investigated.

3. TECHNICAL APPROACH SUMMARY

During this period the second iteration theoretical calculations performed to characterize doubly rotated cuts of quartz were completed. Theoretically temperature stable cuts with zero $TCF^{(1)}$ and $TCF^{(2)}$ as small as -0.93×10^{-8} were located. This represents a four-fold improvement over the ST cut. Experimental measurements of the TCF's have been performed on some doubly rotated cuts. Zero $TCF^{(1)}$ SAW devices for which the second order temperature term is the dominant term have been fabricated. Measured values of $TCF^{(2)}$ of these devices as low as -1.0×10^{-8} have been obtained. The agreement between the experimental and the calculated results was excellent.

To accurately characterize the properties of doubly rotated quartz, this program has utilized two basic theoretical approaches for the identification of zero TCF's. Two computer programs available at Motorola are used. The first program calculates the first, second and third order TCF's of rotated cuts using a finite difference method.[1] This technique is simple, well established, and has been used for analytically determining the temperature coefficient curves for singly and doubly rotated cuts of quartz. To more accurately determine the first order temperature coefficient of frequency, a second program which encompasses lattice skewing effects is used. This more complete theoretical approach is based on the work of Sinha and Tiersten.[2] Its utility has been verified. The characterization of the other key parameters is achieved with standard SAW programs used routinely for material characterization and device development.

Accurately oriented quartz bars, supplied by Motorola Carlisle, are cut and oriented at Motorola and polished at Crystal Technology. During this program, many substrates are fabricated from a single bar with incremental angular deviations about selected angular positions. The angular orientation of the doubly rotated substrates is defined to an accuracy of within ±5 minutes using X-ray diffractometry and precision wafer saw's with doubly rotating mounts.

A complete SAW test area and optical laboratory form the basis for the experimental evaluation of the key SAW parameters of the doubly rotated quartz delay lines, oscillators and resonators. The equipment is set up for rapid display, measurement and recording of propagation directions, TCF's, velocities, beam steering angles and diffraction. Measurement techniques and device designs which minimize the phase distortion in the feedback loop are emphasized to obtain accurate measurements. These include the use of the wide operative output transducer to allow for the power flow angle variation versus temperature and the use of semirigid cables to reduce stray capacitance variation due to vibration.

The excellent agreement between the experimental and theoretical results, and the success with which low TCF cuts have been located, confirmed the utility and accuracy of the techniques used in the program. The second experimental iteration promises to yield devices with even greater temperature stability than those already obtained.

---

[1] "Numerical Computation of Acoustic Surface Waves in Layered Piezoelectric Media-Computer Program Descriptions", William Jones, William Smith, Donald Perry, Final Report F19628-70-C-0027, prepared for Air Force Cambridge Research Laboratories by Hughes Aircraft Company.

[2] "On The Temperature Dependence of the Velocity of Surface Waves in Quartz", B.K. Sinha and H.F. Tiersten, Proceedings of the 32nd Annual Symposium of Frequency Control, 1978, pp. 150-153.

SECTION II

TECHNICAL DISCUSSION

1. INTRODUCTION

The search for a temperature stable cut of quartz for application to SAW devices has lead to the investigation of the doubly rotated cuts. Theoretical studies have indicated that doubly rotated cuts of quartz promise much better temperature stability than the commonly used ST cut. The first iteration of this program, which encompassed the Task I calculations of the doubly rotated cuts of quartz, and the Task II experimental work, have been successfully completed. The second iteration calculations and analysis have also been completed. The second iteration of Task II work is in progress.

In Task I, theoretical analyses have been performed and angular rotations promising very low $TCF^{(1)}$ and $TCF^{(2)}$ have been plotted. Important SAW device design parameters, such as coupling coefficient, velocity and power flow angle, have also been computed to characterize each area. As part of Task II, experimental results establishing the degree of correlation with theory have been obtained.

Theoretical calculations have been in good agreement with experimental results. Doubly rotated cuts of quartz with an improvement of $TCF^{(2)}$ by at least a factor of two over the ST cut have been obtained. A further improvement is expected after a second iteration has been completed and promising areas experimentally examined.

Paragraph 2 presents experimental determination of propagation characteristics which illustrate an excellent agreement between theoretical calculation and experimental results. It also contains the results of the doubly rotated cut TCF measurements made to date. In Paragraph 3 the second iteration theoretical results are presented. Doubly rotated cuts with superior temperature characteristics to those discovered in the first iteration are presented. In Paragraph 4 the temperature variation of the power flow angle and a new mask design insensitive to this variation are discussed.

2. EXPERIMENTAL RESULTS

In the second interim report, experimental results were presented demonstrating the good agreement with the theory. In this third interim period, additional experimental work has been performed. The results of the experimental work performed are summarized in Table 1. The orientations of Table 1 are expressed in the notation of the IRE 1949 standards[3] and were obtained by selecting measurements with zero first-order temperature coefficients of frequency. This was done to ease the comparison between the experimental and theoretical results because these angles can be accurately calculated theoretically, and because it is a

[3]"Standards on Piezoelectric Crystals 1949", Pro. IRE 14, Dec. 1949, pp. 1378-1395.

necessary condition for low TCF orientation. A more accurate measurement of the second-order temperature coefficient of frequency usually results when the first-order coefficient is small. As was noted in the previous interim report, the experimental and calculated results, as can be seen from Table 1, have maintained their high degree of accuracy.

Figure 1 shows a typical frequency-temperature curve used to generate the data in Table 1. The stars represent experimental data points. The solid lines are linearly regressed curves used to define the measured first-, second-, and third-order TCF's for these cuts found in the table. The first order temperature coefficient is small enough so that only a light mask rotation is required to arrive at an orientation with a zero TCF[1]. This small rotation is not enough to significantly change the second-order TCF. Experimental devices with a near zero first-order TCF and a second-order TCF of approximately $-1.0 \times 10^{-8}/C^{o2}$ have been measured. These measured second-order TCF's are significantly lower than the lowest previous measurements of approximately -1.5×10^{-8} with a zero TCF[1]. Figures 2 through 7 are graphs of experimental frequency temperature characteristics of devices fabricated at optimum orientations. Changes in the frequency behavior as a function of mask alignment can be seen clearly.

TABLE 1. COMPARISON OF EXPERIMENTAL AND CALCULATED RESULTS

ANGLES			CALCULATED				MEASURED		
PHI	THET	PSI	TCF^1††	TCF^1†††	TCF^2†††	TCF^3†††	TCF^1	TCF^2	TCF^3
0	42.75	0†	-0.07×10^{-5}	0.06×10^{-5}	-0.40×10^{-7}	0.11×10^{-10}	-0.1×10^{-5}	-0.37×10^{-7}	-0.17×10^{-10}
8.05	25.9	135.7	-0.01	0.74	-0.15	0.42	0.16	-0.16	0.58
6.57	26.88	134.9	-0.24	0.55	-0.15	0.43	0.025	-0.16	0.47
8.03	26.97	134.6	-0.18	0.60	-0.15	0.46	0.067	-0.13	0.46
7.41	27.83	134.2	-0.26	0.54	-0.15	0.49	-0.08	-0.15	0.63
6.00	26.97	135.8	-0.04	0.75	-0.14	0.46	0.15	-0.13	0.30
5.58	27.83	135.2	-0.15	0.65	-0.14	0.49	0.13	-0.13	0.28
-0.03	26.70	138.9	0.28	1.10	-0.11	0.48	0.43	-0.11	0.49
- 0.13	26.1	137.7	0.06	0.69	-0.11	0.53	0.24	-0.097	0.25
0.633	26.15	137.0	-0.24	0.57	-0.13	0.47	-0.11	-0.15	0.86
-0.967	26.23	138.4	0.01	0.82	-0.12	0.51	0.34	-0.13	0.79

†WAFER OBTAINED COMMERCIALLY. ANGULAR TOLERANCE IS UNKNOWN.
††CALCULATED USING SINHA AND TIERSTEN'S PROGRAM.
†††CALCULATED USING FINITE DIFFERENCE APPROACH.

3. THEORETICAL RESULTS

The first iteration results, described in paragraph 2 and in previous reports, were utilized in this period to refine the theoretical results obtained earlier. The close agreement between theory and experiment demonstrated earlier prompted a more thorough theoretical search for promising temperature-stable doubly rotated orientations. An attempt to determine optimum orientations was felt justified in light of the accuracy of the calculated results. Second-order TCF's are predicted by the finite difference method to within 0.005 ppm/C^{o2}. First-order TCF's are predicted to within 3 ppm/C° by the Sinha and Tiersten perturbation method.

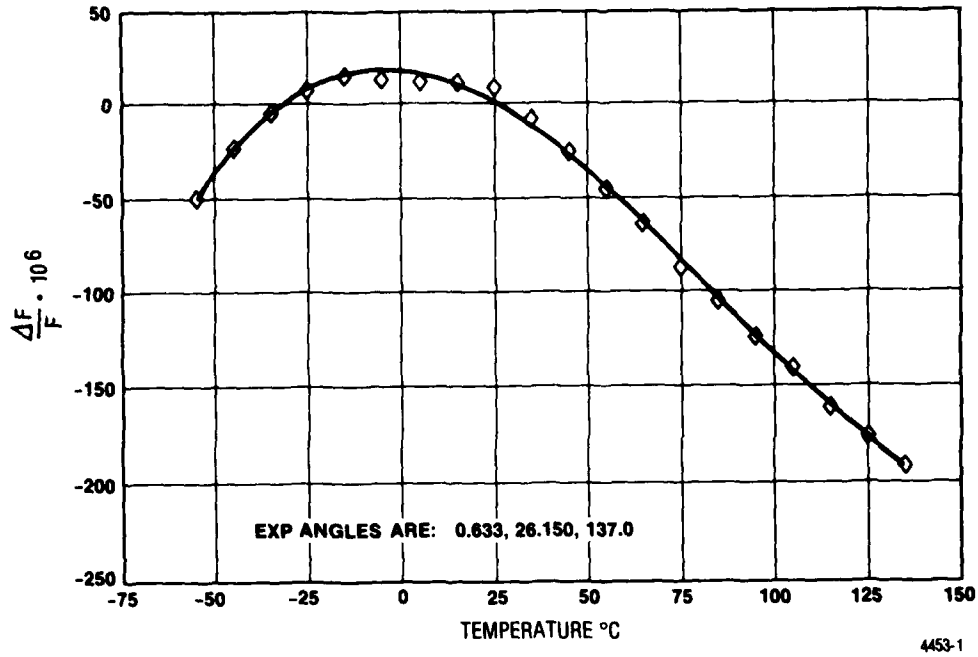

Figure 1. Frequency-Temperature Dependence for (YX wlt) 0.633/26.15/137.0

A more thorough search in and near previously discovered near-optimum orientations did not yield any new results. Other areas previously considered as not quite optimum, on closer examination, were found to have a greater predicted temperature stability than any other orientations yet measured. A second-order TCF of $-0.93 \times 10^{-8}/C^{\circ 2}$ with a zero first-order TCF is predicted for a new family of cuts. The significance of this family of temperature-stable cuts will become evident only after devices are built and experimental results are compared, as the difference in $TCF^{(2)}$'s is about 10 percent. The addition of this family of cuts to our investigation is also significant as it opens up the possibility of selecting cuts not only for improved temperature stability but for improved stress compensation.

Table 2 contains a list of crystal orientations with zero first-order TCF's and low second-order TCF's. Two new families of cuts, centered about (YX wlt) 15°/30°/38° and (YX wlt) 12.5°/35°/130° are included in Table 2. Second-order $TCF^{(2)}$'s of -1.0×10^{-8} and -0.93×10^{-8} are predicted for the two families. Each of the families extends over a surface with a PHI variation of 20° and 15° respectively, and a THETA variation of about 5° and 10° respectively, the PSI angle for obtaining a zero $TCF^{(2)}$ being fixed for each PHI and THETA. Figures 8 through 11 show these areas in detail. Both the zero $TCF^{(1)}$ curves calculated by Sinha and Tiersten's perturbation approach and the finite difference method are shown. Overlapping second-order TCF contours are also plotted.

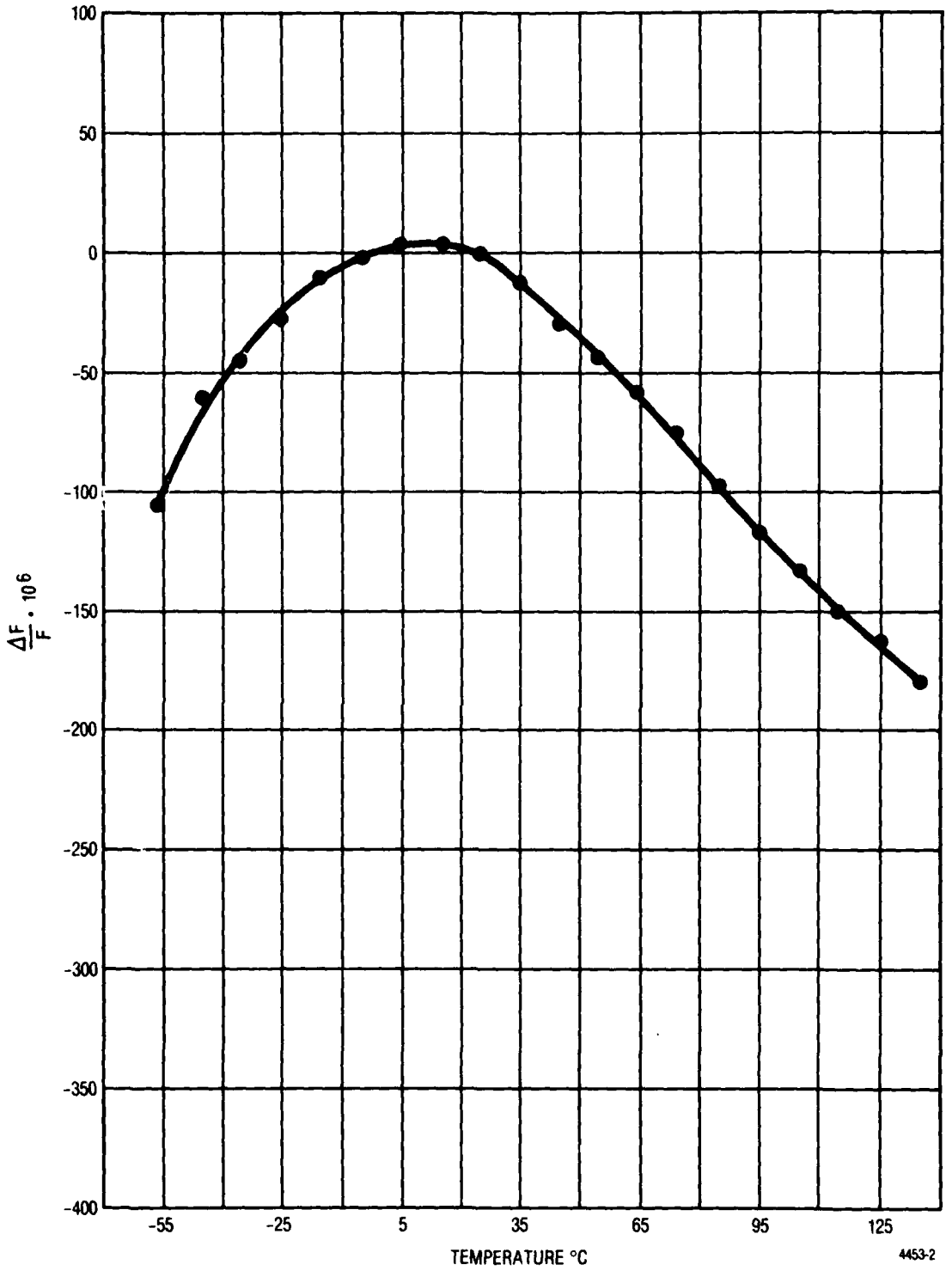

Figure 2. Frequency-Temperature Dependence for (YX wlt)-1.05/28.0667/136.534

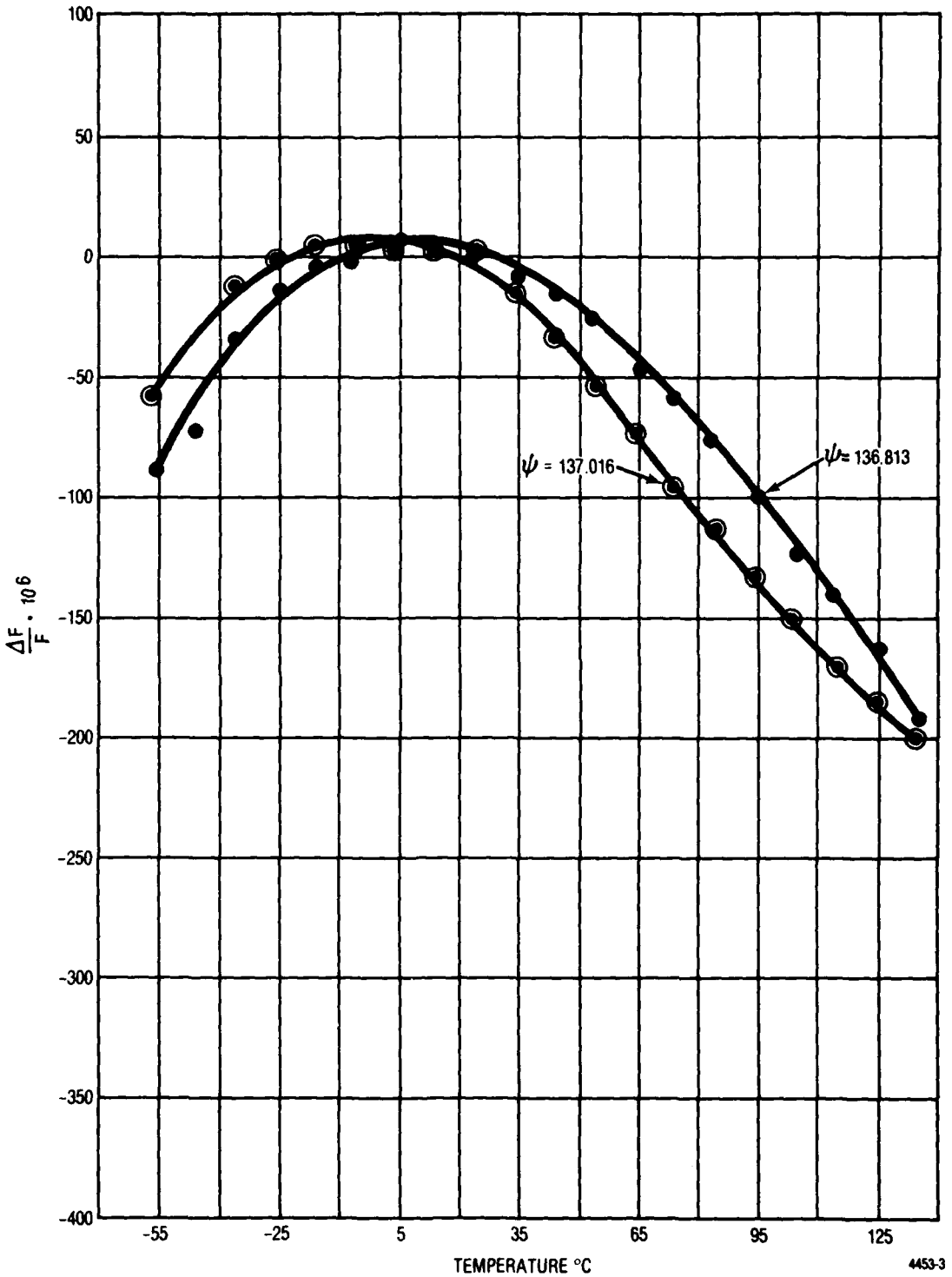

Figure 3. Frequency-Temperature Dependence for (YX wlt) 0.633/26.15/136.813 to (YX wlt) 0.633/26.15/137.016

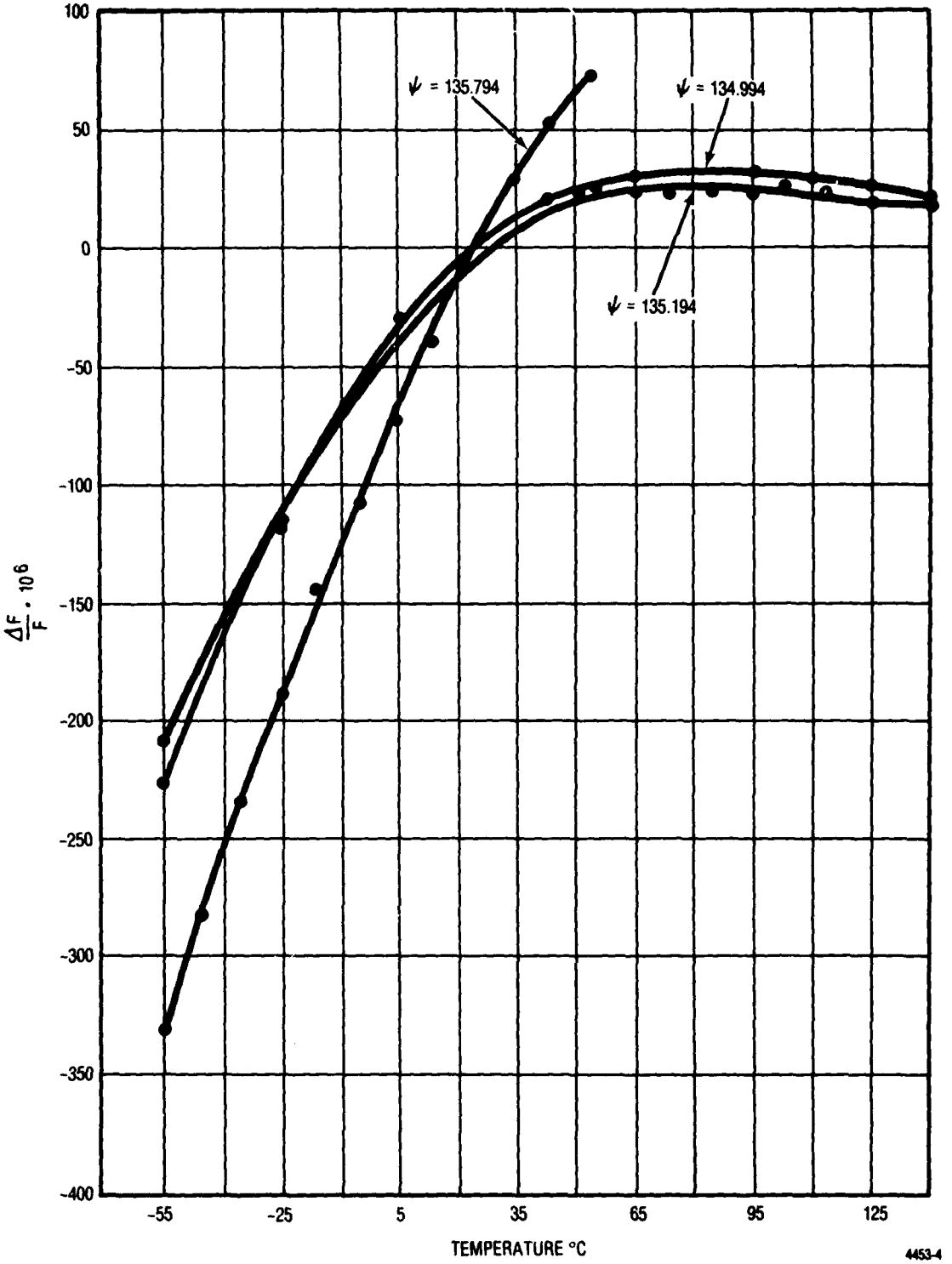

Figure 4. Frequency-Temperature Dependence for (YX wlt) 5.583/27.833/134.994 to (YX wlt) 5.583/27.833/135.794

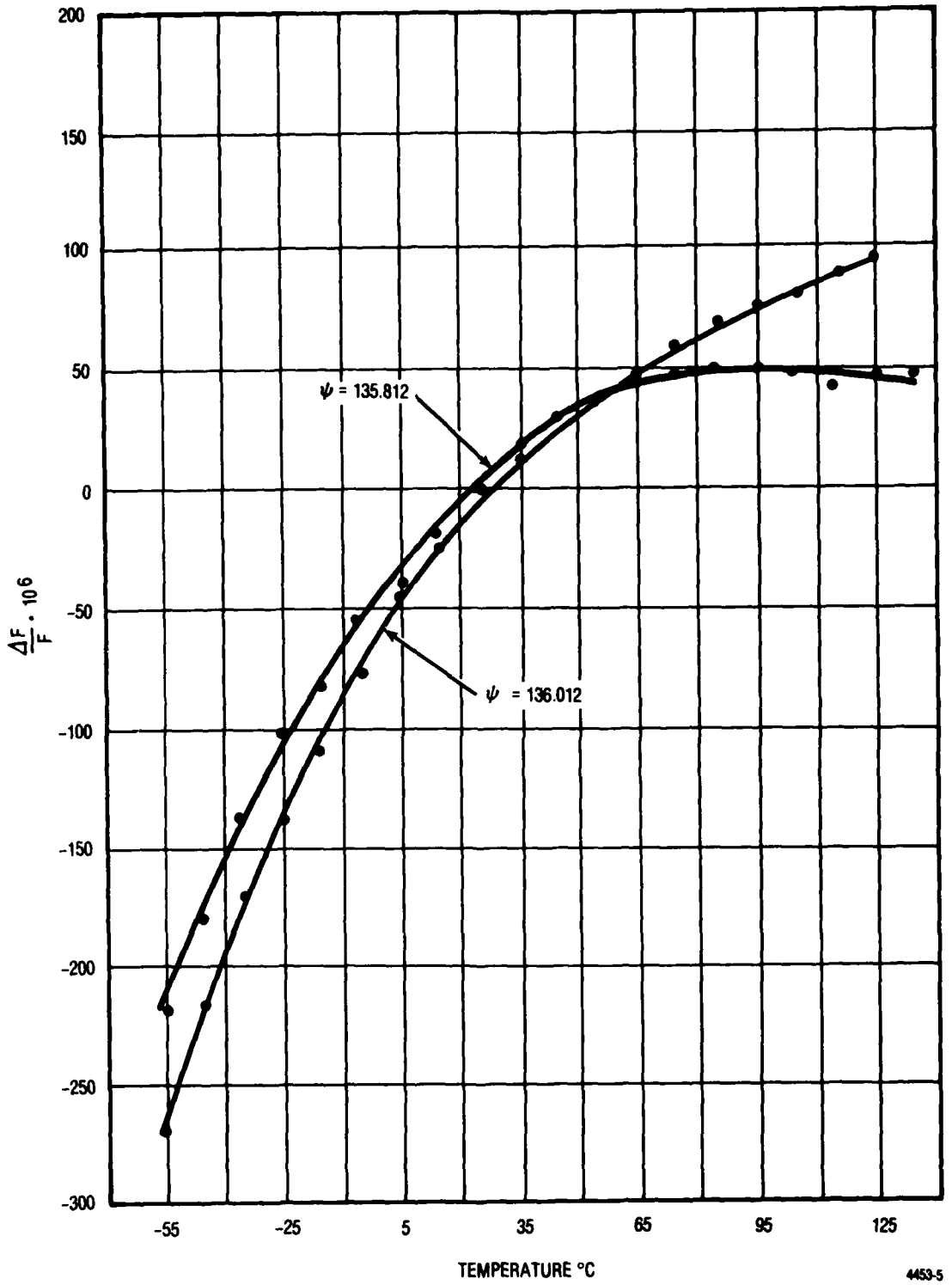

Figure 5. Frequency-Temperature Dependence for
(YX wlt) 6/26.967/135.812 to (YX wlt) 6/26.967/136.012

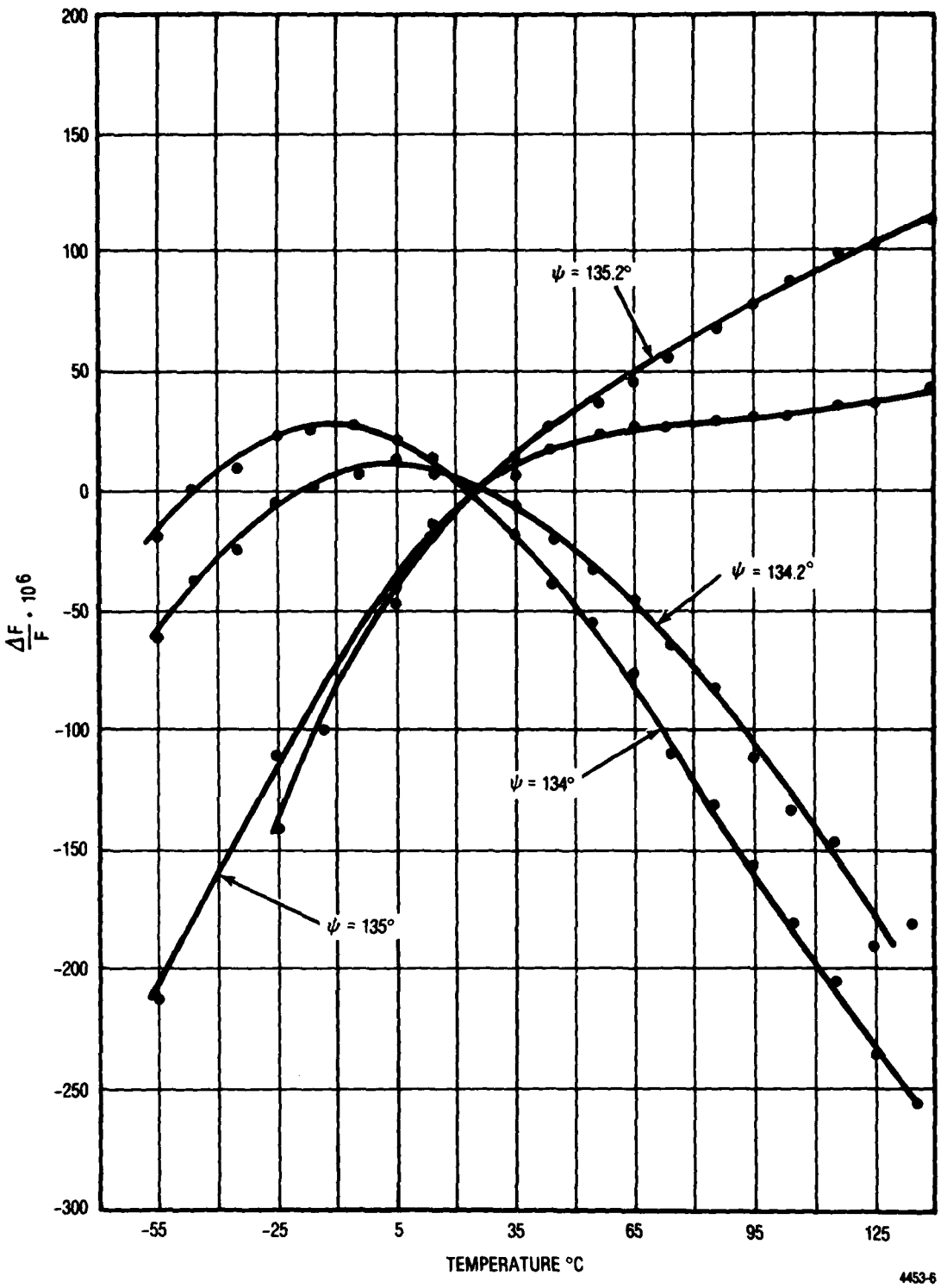

Figure 6. Frequency-Temperature Dependence for (YX wlt) 7.417/27.833/134 to (YX wlt) 7.417/27.833/135.2

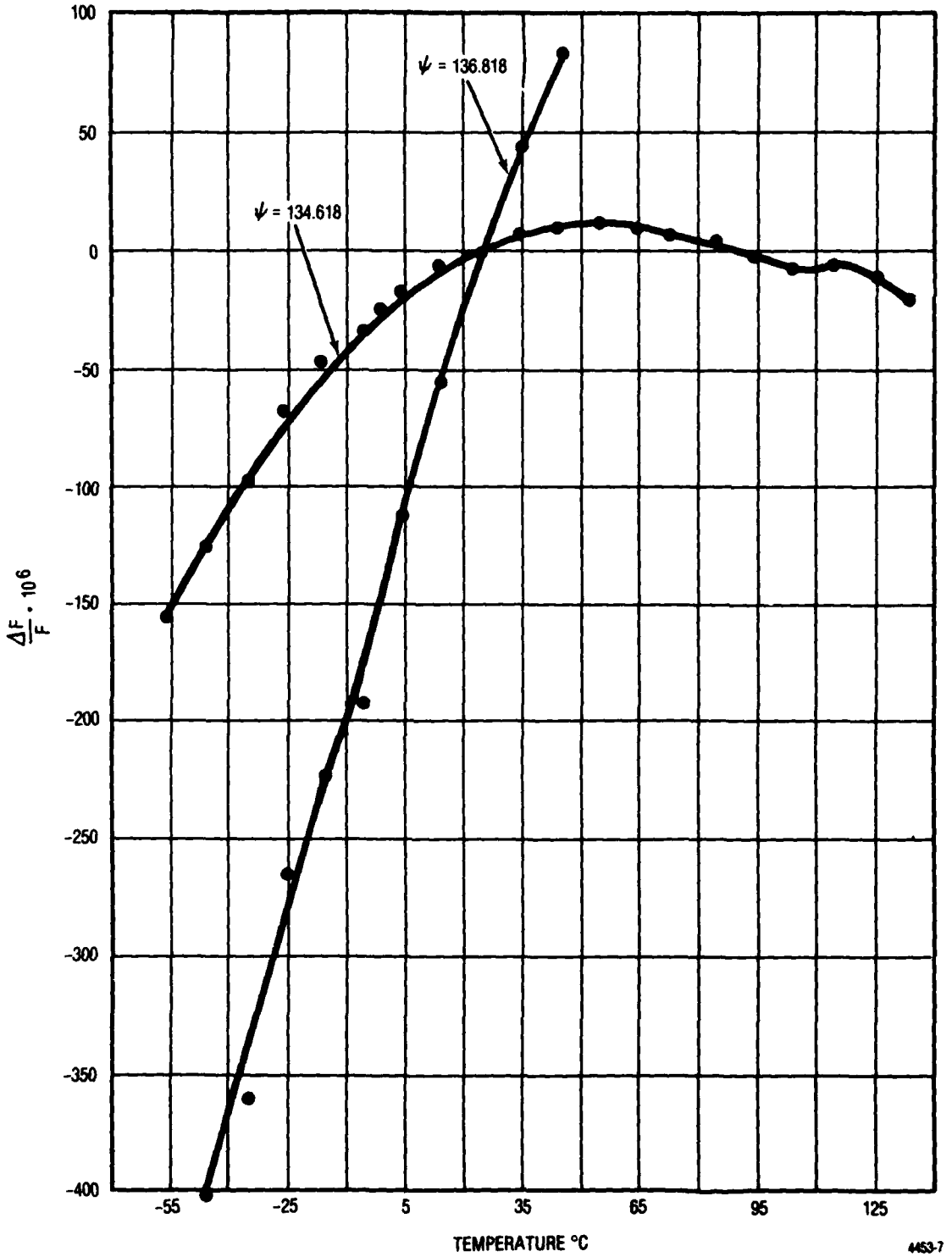

Figure 7. Frequency-Temperature Dependence for (YX wlt) 8.033/26.9667/134.618 to (YX wlt) 8.033/26.9667/136.818

TABLE 2. PROPAGATION CHARACTERISTICS OF CRYSTAL ORIENTATIONS

ANGLES OF ZTCF[1] DEGREES (S AND T'S PROGRAM)			$TCF^{(2)}/°C^2$ ($X10^{-6}$) FINITE DIFFERENCE PROGRAM	$TCF^{(3)}/°C^3$ ($X10^{-10}$) FINITE DIFFERENCE PROGRAM
PHI	THETA	PSI		
6	26	138.31	-1.4	
6	27	135.93	-1.3	0.67
6	28	135.59	-1.3	0.57
7	26	135.99	-1.5	
7	27	135.64	-1.4	
7	28	135.27	-1.3	0.65
8	26	135.74	-1.4	0.65
8	27	135.36	-1.4	
8	28	134.97	-1.3	
1	26	137.78	-1.2	0.68
1	27	137.46	-1.2	0.65
1	28	137.17	-1.1	0.67
0	26	138.07	-1.2	0.67
0	27	137.78	-1.1	0.68
0	28	137.49	-1.1	0.62
-1	26	138.37	-1.2	0.60
-1	27	138.09	-1.2	0.62
-1	28	137.80	-1.1	0.73
14	39	40.195	-1.0	0.64
14	40	40.415	-1.0	0.66
14	41	40.64	-1.0	0.75
15	39	39.79	-1.0	0.63
15	40	40	-1.0	0.74
15	41	40.23	-1.0	0.73
16	39	39.4	-1.0	0.68
16	40	39.605	-1.0	0.66
16	41	39.825	-1.1	0.60
7.5	35.0	41.77	-0.95	0.58
10	35	40.82	-0.94	0.58
12.5	30	38.88	-0.93	0.57
12.5	32.5	39.4	-0.93	0.57
15.0	30.0	38.12	-0.93	0.57
15.0	32.5	38.55	-0.93	0.57
17.5	30.0	37.35	-0.94	0.56
20.0	30.0	36.6	-0.97	0.55
22.5	30.0	35.85	-1.0	0.54
25.0	30.0	35.07	-1.0	0.52
27.5	30.0	34.26	-1.1	0.50
7.5	35.0	132.68	-1.1	0.54
10.0	40.0	129.4	-1.1	0.57
12.5	35.0	130.62	-1.0	0.41
12.5	42.5	127.15	-1.1	0.58
15.0	45.0	124.43	-1.1	0.58
17.5	40.0	126.14	-1.1	0.54
20.0	40.0	124.92	-1.0	0.44

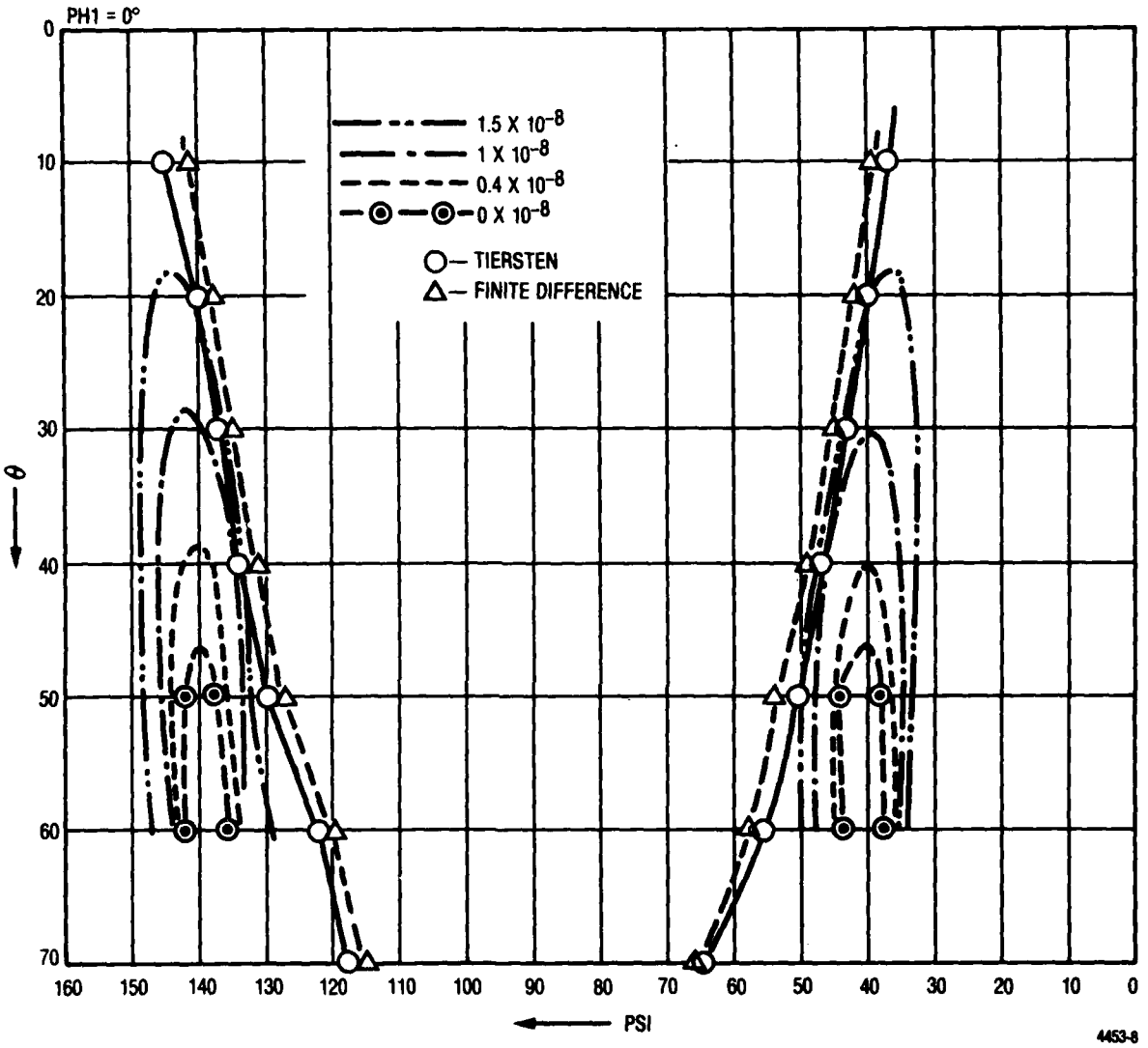

Figure 8. TCF Contour Map (PHI = 0°)

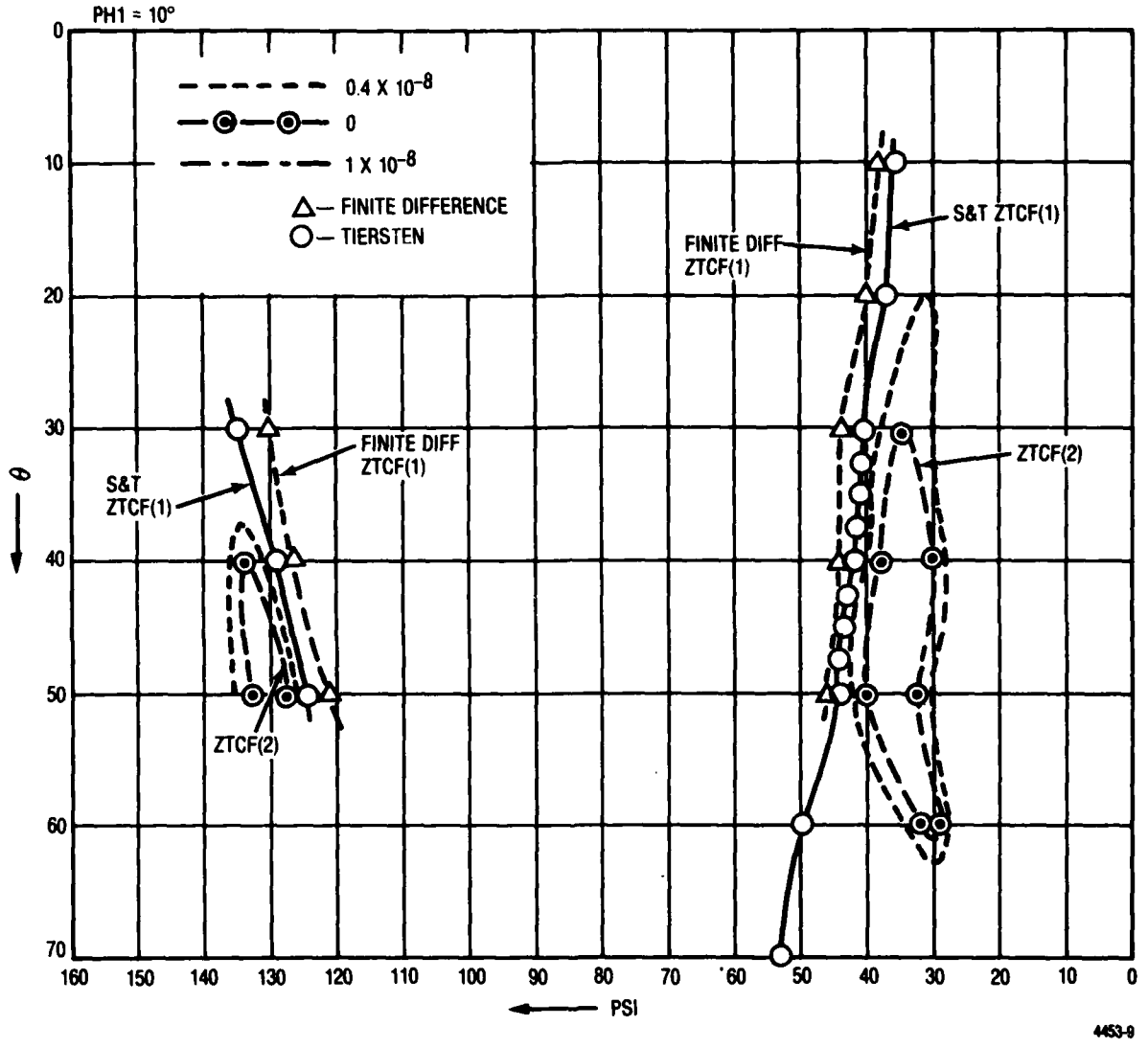

Figure 9. TCF Contour Map (PHI = 10°)

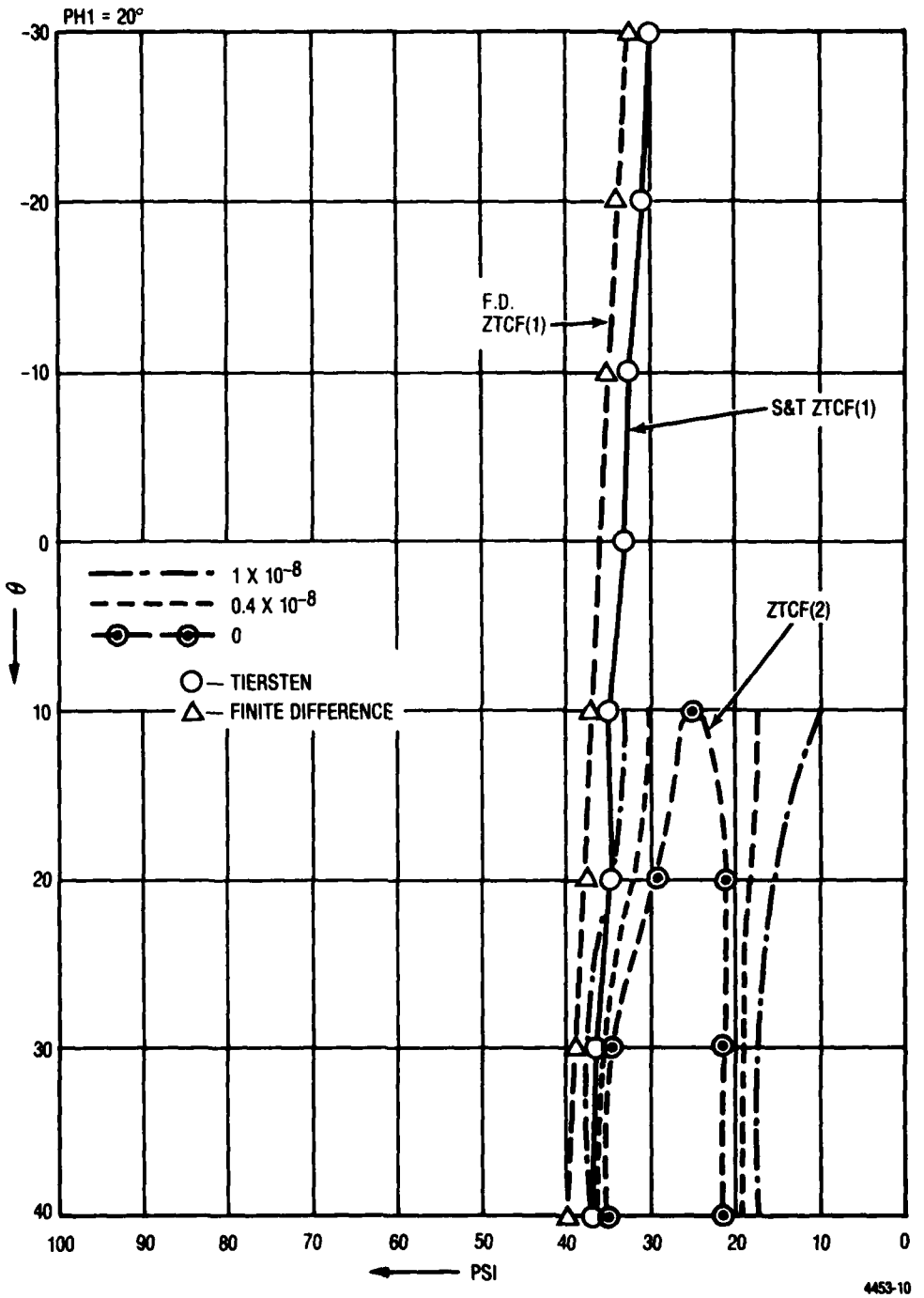

Figure 10. TCF Contour Map (PHI = 20°)

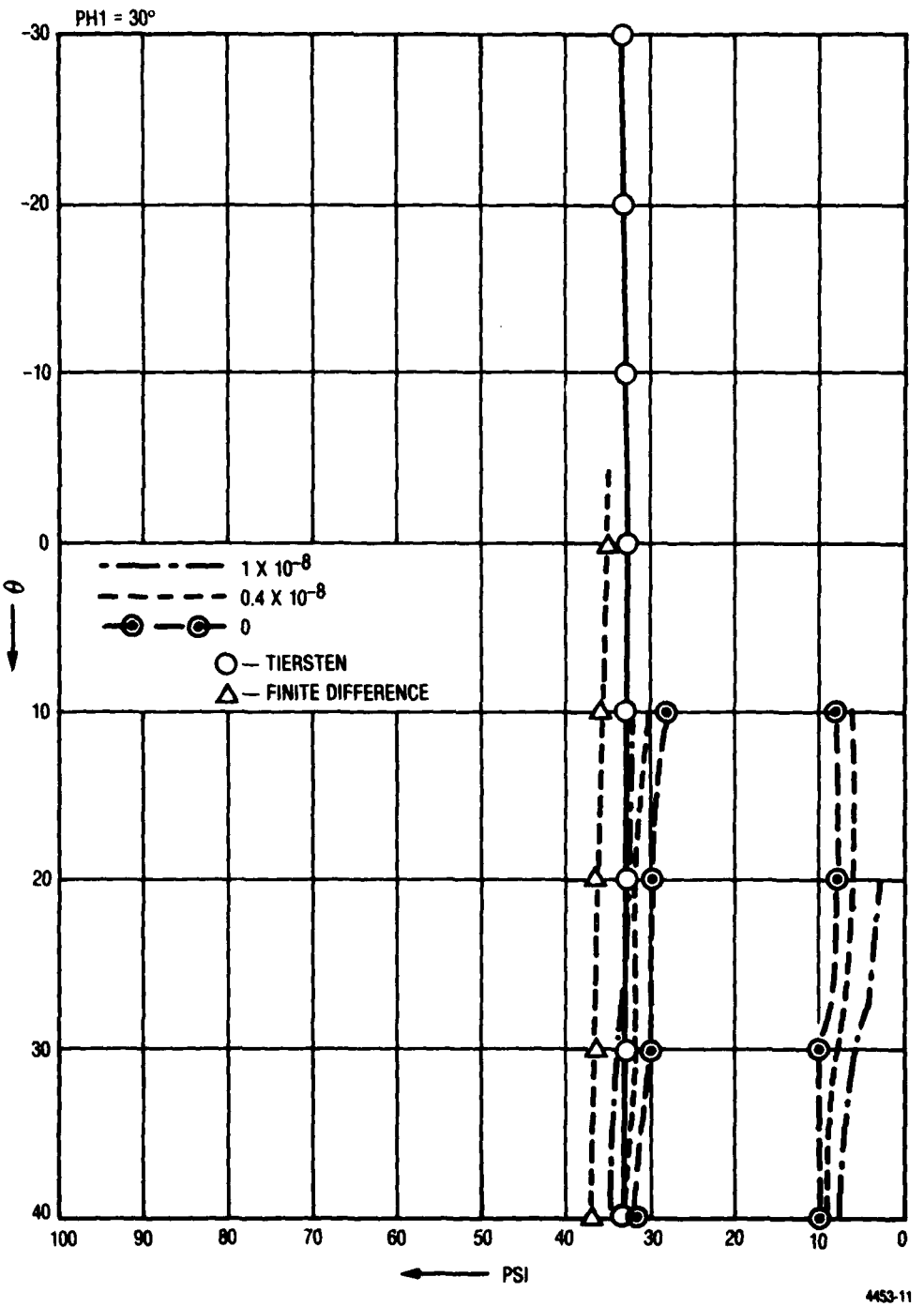

Figure 11. TCF Contour Map (PHI = 30°)

Table 3 contains some of the propagation characteristics of these selected orientations. The velocities, coupling coefficients, and power flow angles are seen to be quite reasonable. Tables 4 and 5 contain the derivatives of the first-order temperature coefficients of frequency with respect to angular changes in orientation. These derivatives determine the accuracy with which one must fabricate to ensure a negligable $TCF^{(1)}$. The nonzero value of $\partial TCF^{(1)}/\partial\phi$ allows a compensation for misalignment of the wafer orientation by a compensation in mask orientation as the values of $\partial TCF^{(2)}/\partial\phi$, $\partial TCF^{(2)}/\partial\theta$, and $\partial TCF^{(2)}/\partial\psi$ are small. In the first iteration of Task II, it was demonstrated that devices with these $TCF^{(1)}$ angular derivatives are easily fabricated with low $TCF^{(1)}$. These two families of cuts are believed to be entirely suitable to temperature-stable SAW device fabrication.

TABLE 3. PROPAGATION CHARACTERISTICS OF SELECTED ORIENTATIONS

ANGLES OF $ZTCF^{(1)}$, DEGREES (S AND T'S PROGRAM)			VELOCITY (MSEC)	K^2 ($X10^{-3}$)	POWER FLOW ANGLE (DEGREES)
PHI	THETA	PSI			
6	26	136.31	3266.84	1.12	-0.3
6	27	136.03	3263.60	1.12	-0.2
6	28	135.58	3260.63	1.12	-0.1
7	26	135.99	3303.33	1.12	-0.5
7	27	135.64	3299.70	1.12	-0.4
7	28	135.27	3296.33	1.12	-0.3
8	26	135.74	3310.15	1.12	-0.7
8	27	135.36	3306.11	1.12	-0.6
8	28	134.97	3302.32	1.10	-0.5
1	26	137.78	3268.80	1.10	+0.7
1	27	137.48	3267.44	1.10	+0.9
1	28	137.17	3266.36	1.10	+1.0
0	26	138.07	3264.09	1.12	+0.9
0	27	137.78	3263.09	1.10	+1.1
0	28	137.49	3262.35	1.10	+1.2
-1	26	138.37	3259.65	1.10	+1.1
-1	27	138.09	3259.01	1.10	-1.3
-1	28	137.80	3258.64	1.08	+1.5
14	39	40.195	3298.60	0.96	-7.7
14	40	40.415	3306.67	0.96	-8.1
14	41	40.64	3315.19	0.94	-8.6
15	39	39.79	3301.82	0.96	-7.8
15	40	40.00	3310.14	0.94	-8.3
15	41	40.23	3319.00	0.98	-8.6
16	39	39.4	3305.36	0.96	-8.0
16	40	39.606	3314.03	0.98	-8.4
7.5	36.0	41.77	3262.43	1.00	-4.8
10	36.0	40.82	3264.23	1.01	-5.3
12.5	36.0	39.86	3243.27	1.01	-4.1
12.5	32.5	39.4	3254.49	1.00	-4.9
15.0	30.0	38.12	3244.98	0.98	-4.6
15.0	32.5	38.56	3257.82	0.98	-5.3

TABLE 4. $\partial TCF^{(1)}/\partial\psi$ FOR SELECTED CUTS

Angles of $ZTCF^{(1)}$, Degrees (S and T'S Program)			$\partial TCF^{(1)}/\partial\psi$
PHI	THETA	PSI	
6	26	136.31	+2.7 (PPM/C°)/DEGREE
6	27	135.93	+2.7
6	28	135.59	+2.7
7	26	135.99	+2.7
7	27	135.64	+2.7
7	28	135.27	+2.7
8	26	135.74	+2.7
8	27	135.36	+2.7
8	28	134.97	+2.7
1	26	137.78	+2.8
1	27	137.48	+2.8
1	28	137.17	+2.8
0	26	138.07	+3.0
0	27	137.78	+3.0
0	28	137.49	+3.0
−1	26	138.37	+3.0
−1	27	138.09	+3.0
−1	28	137.08	+3.0
14	39	40.195	−3.5
14	40	40.415	−3.5
14	41	40.64	−3.5
15	39	39.79	−3.5
15	40	40	−3.5
15	41	40.23	−3.5
16	39	39.4	−3.7
16	40	39.605	−3.7
16	41	39.825	−3.7
7.5	35.0	41.77	−3.3
10.0	35.0	40.82	−3.4
12.5	30.0	38.88	−3.3
12.5	32.5	39.4	−3.2
15.0	30.0	38.12	−3.4

TABLE 4. $\partial TCF^{(1)}/\partial\psi$ FOR SELECTED CUTS (CONT)

Angles of $ZTCF^{(1)}$, Degrees (S and T'S Program)			$\partial TCF^{(1)}/\partial\psi$
PHI	THETA	PSI	
15.0	32.5	38.55	–3.6
17.5	30.0	37.35	–3.4
20.0	30.0	36.6	–3.5
22.5	30.0	35.85	–3.5
25.0	30.0	35.07	–3.3
27.5	30.0	34.28	–3.4
7.5	35.0	132.68	+2.7
10.0	40.0	129.40	+2.8
12.5	35.0	130.62	+2.0
12.5	42.5	127.15	+2.5
15.0	45.0	124.43	+2.6
17.5	40.0	126.14	+2.1
20.0	40.0	124.92	+2.6

TABLE 5. $\partial TCF^{(1)}/\partial\phi$ AND $\partial TCF^{(1)}/\partial\theta$ FOR SELECTED CUTS

Angles of $ZTCF^{(1)}$, Degrees (S and T's Program)			$\partial TCF^{(1)}/\partial\phi$	$\partial TCF^{(1)}/\partial\theta$
PHI	THETA	PSI		
7	27	135.64	–0.7 (PPM/C°)/DEGREE	–0.5 (PPM/C°)/DEGREE
0	27	137.78	–0.8	–0.8
15	40	40.00	+1.5	–0.7
15.0	32.5	38.55	–1.2	0.6
12.5	35.0	130.62	0.95	1.1

4. TEMPERATURE VARIATION OF THE SAW POWER FLOW ANGLE

An unexpected rapid fluctuation of the surface acoustic wave power flow angle on doubly rotated cut quartz saw devices was discovered during the testing of temperature-stable SAW devices. In this paragraph the phenomenon of a temperature variation in the SAW power flow angle will be discussed.

The power flow angle for a particular direction of propagation is an important parameter. While the phase fronts always remain parallel to the source transducer, the wave as a whole does not propagate

perpendicular to the wavefronts. This is a characteristic of anisotropic substrates where the phase velocity is asymmetric about the propagation direction; i.e. $\nu(\psi + \Delta\psi) \neq \nu(\psi - \Delta\psi)$. The major problem which arises is that the acoustic beam may steer off the desired propagation track missing the output transducer unless it is properly designed.

The power per unit width carried in a surface wave is found by integrating the mechanical and electrical Poynting vectors, to obtain

$$P_i = -\frac{1}{2}\mathrm{Re}\left[\int_{-\infty}^{0} T_{ij}\mu_j^* \, dx_3 - i\omega\int_{-\infty}^{\infty} \phi D_i \, dx_3\right] \qquad (i = 1, 2)$$

where μ_i is the particle displacement, T_{ij} the stress tensor, ϕ the electric potential and D_i the electric displacement. P_1 and P_2 give the power flow perpendicular and parallel to the wavefront, respectively. $P_3 = 0$ for the Rayleigh wave which is confined to the surface. The power flow angle may be defined as $\theta = \arctan(P_2/P_1)$. Power flow angles as high as 20° are not uncommon on quartz.

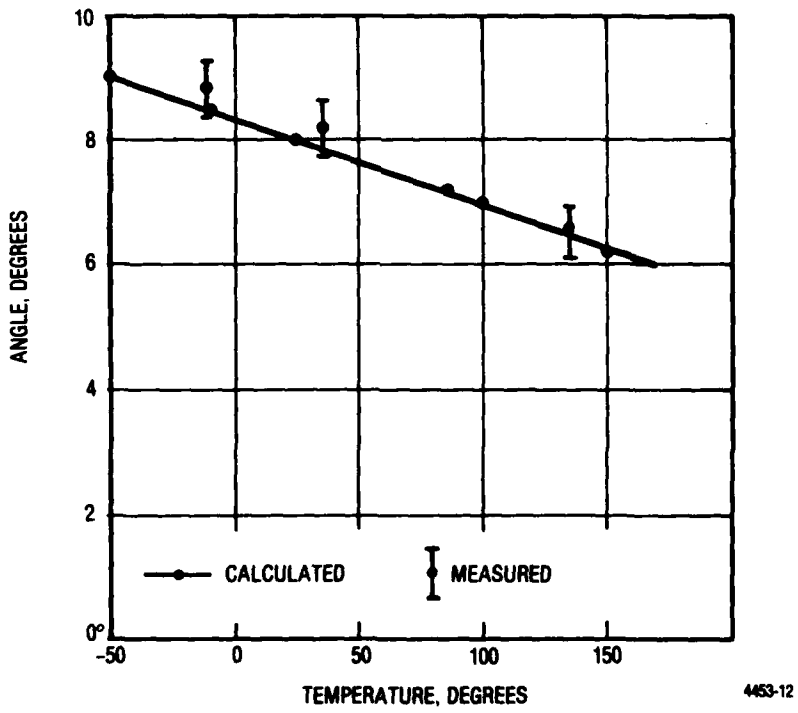

Figure 12. Power Flow Angle Against Temperature for (YX wlt) 14·283/39·117/40·6

Calculations[3,4] of the power flow angle at different temperatures for doubly rotated cuts of quartz have been performed. The cuts are designated by the 1949 IRE[3] standard. Figure 12 illustrates the temperature variation of the power flow angle for the doubly rotated cut of quartz (YX wlt) 14·283/39·117/40·6. The important feature of this dependence is the large variation of the power flow angle over the temperature range shown.

Figure 13 contains a pictorial representation of a device fabricated at (YX wlt) 14·3/39·1/40·6. The input transducer on the left generates an acoustic wave which only partially illuminates the output transducer on the right. Figure 14 (a and b) are photographs of the device response with a short gated RF pulse as the input, showing the response at 131°C and 34°C, respectively. The first notch is a result of missing finger pairs. The anisotropy parameter[5] was calculated to be 0·625 at –50°C, 0·614 at 25°C and 0·586 at 150°C. The transducer apertures are 34 mils and 24 mils, the length of the device is 260 mils and the acoustic wavelength is 0·48 mils. The temperature dependent effects of diffraction on the envelope were found to be negligible. The shortening of the device response is clearly evident from the photographs and is due to the rapidly decreasing power flow angle successively illuminating more of the output transducer as the temperature increases. The power flow angles estimated from these photographs are displayed in Figure 8, alongside the theoretical results. Table 6 contains a summary of the power flow angles temperature dependence for several temperature-stable doubly rotated cuts.

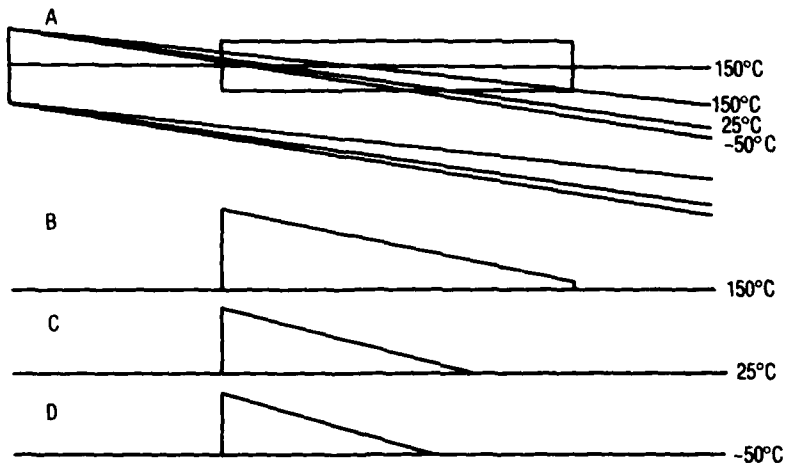

A. DEVICE GEOMETRY
B. IMPULSE RESPONSE AT 150°C
C. IMPULSE RESONSE AT 25°C
D. IMPULSE RESPONSE AT -50°C

4453-13

Figure 13. Pictorial Representation of Device Response

[4]"Higher Order Temperature Coefficients of the Elastic Stiffness and Compliances of Alpha-Quartz", Bechmann, R., Ballato, A., and Lukaszek, T., IRE Trans., 1962, pp. 1812-1822.

[5]"Compensation for Diffraction in SAW Filters", Savage, E. B., and Matthaei, G. L., 1979 IEEE Ultrasonics Symposium, CH1482-9/79/, pp. 527-532.

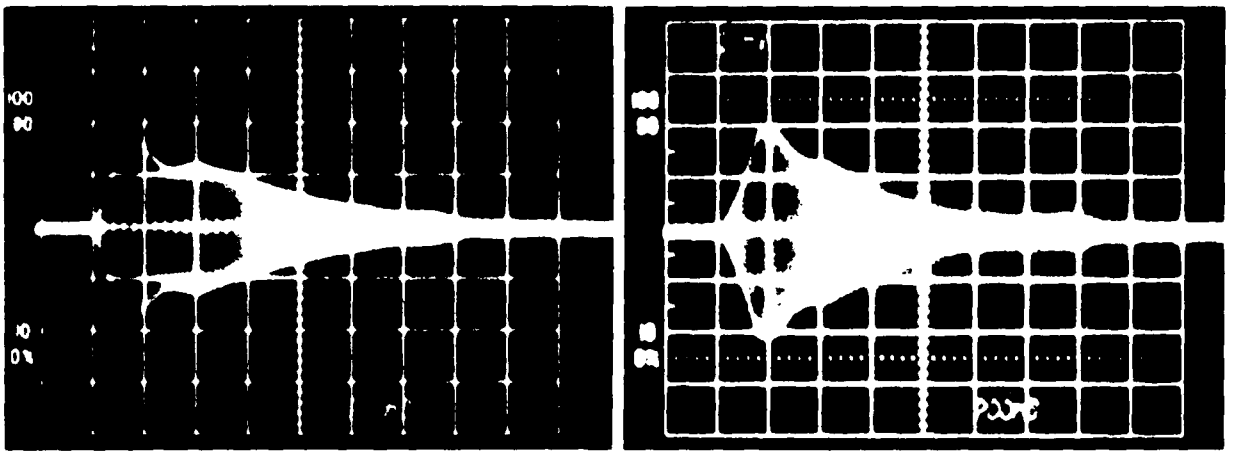

a. AT 131°C b. AT 34°C

4523-4

Figure 14. Device Response to Short Gated 270-4 MHz Input Pulse

TABLE 6. TEMPERATURE DEPENDENCE OF THE POWER FLOW ANGLE ON DOUBLY ROTATED CUTS AT ORIENTATIONS (YX WLT) PHI/THETA/PSI

Orientation			Power Flow Angle		
PHI	THETA	PSI	T = 25°C	T = 150°C	T = −50°C
−1.330	28.100	137.692	+1.2	−0.1	+1.8
−1.050	28.067	136.534	+2.5	+1.0	+3.2
−0.967	26.233	138.449	+1.1	−0.2	+1.8
−0.33	26.700	138.859	+0.5	−0.7	+1.1
0.633	26.150	137.016	+1.4	+0.1	+2.1
5.583	27.833	135.194	+0.3	−0.9	+1.0
5.583	27.833	134.940	+0.5	+0.1	+1.1
5.583	27.833	134.994	+0.4	−0.8	+1.1
6.000	26.967	135.812	−0.1	−1.2	+0.5
6.067	25.933	133.099	+1.7	+0.3	+2.4
6.567	26.883	134.925	+0.1	−1.0	+0.7
7.410	27.380	134.2	+0.1	−1.0	+0.8
8.033	26,967	134.618	−0.3	−1.4	−0.3
8.05	25.900	135.71	−0.7	−1.6	−0.1
14.283	39.117	40.627	−8.1	−6.2	−9.0
15.300	40.683	40.031	−8.6	−6.8	−9.6
16.117	41.267	37.309	−7.2	−5.5	−8.1

When the oscillator frequency is not exactly at the synchronous frequency of the SAW delay line, the phase response of the delay line becomes temperature dependent. The use of doubly rotated cut SAW devices clearly requires designs which can accommodate a large variation in the SAW power flow angle. Consequently, a special mask used for testing was designed.

Figure 15 contains an illustration of the pattern to be used for doubly rotated cuts with a large power flow angle temperature variation. The large aperture of the output transducer is required to accommodate rapid variation of the power flow angle.

The center frequency of the device is approximately 260 MHz. The electrode and line spacing are 0.06 mil (double electrodes), so the acoustic wavelength is 0.48 mil. The input transducer has 40 pairs of electrodes and the output transducer has 11 sections of electrodes with 4.5 pairs in each section. The spacing of each section is 19.2 mils. The width of the input transducer is 36 mils, and that for the output transducer is 120 mils. The design allows a maximum of 12 degrees beam steering, which is adequate for most of the desired cuts in this study. The final mask is a stepped and reduced design having a family of patterns with relative rotation of a fraction of a degree, so that a family of TCF's with small increments of the propagation angle 0.4° can be measured.

The input transducer is divided into two sections. Selecting the upper or lower section ensures that the complete wavefront of the acoustic waves will propagate over the output transducer aperture throughout the temperature range of interest.

In designing filters and reflective array devices on rotated cuts of quartz, additional care must be taken to ensure that the temperature dependent power flow angle does not degrade device response. If improperly designed, device time delay, bandwidth and phase all become temperature dependent when fabricated on a rotated cut. These observations are especially important for reflective array devices in which rotated cuts of quartz are often used to achieve temperature compensation in two different propagation directions. Suitable device design can overcome these problems and result in temperature compensated delay lines useful for oscillator applications. The moving acoustic beam may be made to illuminate different parts of the output transducer at different temperatures in such a way as to maintain a steady phase over the entire temperature range. A design using the temperature dependent PFA is currently being fabricated in which a compensation signal maintains a relatively constant output phase despite the temperature dependent delay time. Input beam aperture compression may be used to achieve increasingly accurate adjustments of the output phase. Materials such as lithium niobate with higher coupling coefficients may be useful in this respect.

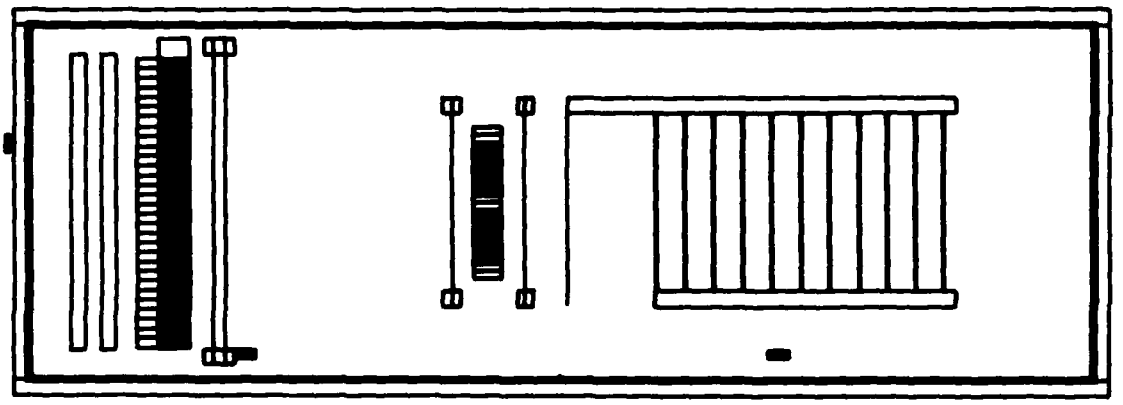

4453-17

Figure 15. Transducer Design

SECTION III

CONCLUSION

Additional experimental results have shown continued agreement with theoretical calculations. Doubly rotated devices with second-order temperature coefficients of frequency as small as -1.0×10^{-8} have been fabricated and tested. These devices are over three times as stable as the ST cut.

The second iteration of analytical evaluation yielded two new temperature-stable families of cuts, one with optimum orientation possessing the lowest second-order temperature coefficient of frequency yet predicted in quartz. For several orientations, a $TCF^{(2)} = -0.93 \times 10^{-8}$ is predicted.

The temperature variation of the power flow angle on doubly rotated cuts of quartz and its effect on device design was discussed. An oscillator design accommodating large temperature-varying power flow angles was discussed. The utilization of the temperature variation of the power flow angle to achieve temperature compensation of the oscillator was suggested.

BIBLIOGRAPHY

1. SLOBODNIK, A. J., DELMONICO, R. T., and CONWAY, E. D.: 'Microwave acoustics handbook'. Air Force Cambridge Research Laboratories, Report #PSRP 609
2. SCHULZ, B.: 'Surface acoustic wave delay lines with small temperature coefficient', *Proc. IEEE*, 1970, pp. 1361-1362

ELECTRONICS TECHNOLOGY AND DEVICES LABORATORY
MANDATORY CONTRACT DISTRIBUTION LIST

101 Defense Technical Information Center
ATTN: DTIC-TCA
Cameron Station (Bldg 5)
012 Alexandria, VA 22314

203 GIDEP Engineering & Support Dept
TE Section
PO Box 398
001 NORCO, CA 91760

205 Director
Naval Research Laboratory
ATTN: CODE 2627
001 Washington, DC 20375

301 Rome Air Development Center
ATTN: Documents Library (TILD)
001 Griffiss AFB, NY 13441

437 Deputy for Science & Technology
Office, Asst Sec Army (R&D)
001 Washington, DC 20310

438 HQDA (DAMA-ARZ-D/Dr. F.D. Verderame)
001 Washington, DC 20310

482 Director
US Army Materiel Systems Analysis Actv
ATTN: DRXSY-MP

001 Aberdeen Proving Ground, MD 21005

563 Commander, DARCOM
ATTN: DRCDE
5001 Eisenhower Avenue
001 Alexandria, VA 22333

564 Cdr, US Army Signals Warfare Lab
ATTN: DELSW-OS
Vint Hill Farms Station
001 Warrenton, VA 22186

705 Advisory Group on Electron Devices
201 Varick Street, 9th Floor
002 New York, NY 10014

579 Cdr, PM Concept Analysis Centers
ATTN: DRCPM-CAC
Arlington Hall Station
001 Arlington, VA 22212

602 Cdr, Night Vision & Electro-Optics
ERADCOM
ATTN: DELNV-D
001 Fort Belvoir, VA 22060

603 Cdr, Atmospheric Sciences Lab
ERADCOM
ATTN: DELAS-SY-S
001 White Sands Missile Range, NM 88002

607 Cdr, Harry Diamond Laboratories
ATTN: DELHD-CO, TD (In Turn)
2800 Powder Mill Road
001 Adelphi, MD 20783

609 Cdr, ERADCOM
ATTN: DRDEL-CG, CD, CS (In Turn)
2800 Powder Mill Road
001 Adelphi, MD 20783

612 Cdr, ERADCOM
ATTN: DRDEL-CT
2800 Powder Mill Road
001 Adelphi, MD 20783

680 Commander
US Army Electronics R&D Command
000 Fort Monmouth, NJ 07703
1 DELET-MQ
1 DELEW-D
1 DELET-DD
1 DELSD-L (Tech Library)
2 DELSD-L-S (STINFO)
34 Originating Office
1 DELET-MF

681 Commander
US Army Communications R&D Command
ATTN: USMC-LNO
001 Fort Monmouth, NJ 07703

ELECTRONICS TECHNOLOGY AND DEVICES LABORATORY

SUPPLEMENTAL CONTRACT DISTRIBUTION LIST

(ELECTIVE)

103 Code R123, Tech Library
DCA Defense Comm Engrg Ctr
1800 Wiehle Ave
001 Reston, VA 22090

104 Defense Communications Agency
Technical Library Center
Code 205 (P. A. Tolovi)
001 Washington, DC 20305

206 Commander
Naval Electronics Laboratory Center
ATTN: Library
001 San Diego, CA 92152

207 Cdr, Naval Surface Weapons Center
White Oak Laboratory
ATTN: Library Code WX-21
001 Silver Spring, MD 20910

314 Hq, Air Force Systems Command
ATTN: DLCA
Andrews Air Force Base
001 Washington, DC 20331

403 Cdr, MICOM
Redstone Scientific Info Center
ATTN: Chief, Document Section
001 Redstone Arsenal, AL 35809

406 Commandant
US Army Aviation Center
ATTN: ATZQ-D-MA
001 Fort Rucker, AL 36362

407 Director, Ballistic Missile Defense
Advanced Technology Center
ATTN: ATC-R, PO Box 1500
001 Huntsville, AL 35807

418 Commander
HQ, Fort Huachuca
ATTN: Technical Reference Div
001 Fort Huachuca, AZ 85613

475 Cdr, Harry Diamond Laboratories
ATTN: Library
2800 Powder Mill Road
001 Adelphi, MD 20783

477 Director
US Army Ballistic Research Labs
ATTN: DRXBR-LB
001 Aberdeen Proving Ground, MD 21005

*481 Harry Diamond Laboratories
ATTN: DELHD-RCB (Dr. J. Nemarich)
2800 Powder Mill road
001 Adelphi, MD 20783

482 Director
US Army Materiel Systems Analysis Actv
ATTN: DRXSY-T, MP (In Turn)
001 Aberdeen Proving Ground, MD 21005

507 Cdr, AVRADCOM
ATTN: DRSAV-E
PO Box 209
001 St. Louis, MO 63166

511 Commander, Picatinny Arsenal
ATTN: SARPA-FR-5, -ND-A-4,
-TS-S (In Turn)
001 Dover, NJ 07801

515 Project Manager, REMBASS
ATTN: DRCPM-FFR-TM
001 Fort Monmouth, NJ 07703

517 Commander
US Army Satellite Communications Agcy
ATTN: DRCPM-SC-3
001 Fort Monmouth, NJ 07703

518 TRI-TAC Office
ATTN: TT-SE
001 Fort Monmouth, NJ 07703

*For Millimeter & Microwave Devices Only

ELECTRONICS TECHNOLOGY AND DEVICES LABORATORY
SUPPLEMENTAL CONTRACT DISTRIBUTION LIST (CONT)
(ELECTIVE)

519 Cdr, US Army Avionics Lab
AVRADCOM
ATTN: DAVAA-D
001 Fort Monmouth, NJ 07703

520 Project Manager, FIREFINDER
ATTN: DRCPM-FF
001 Fort Monmouth, NJ 07703

521 Commander
Project Manager, SOTAS
ATTN: DRCPM-STA
001 Fort Monmouth, NJ 07703

531 Cdr, US Army Research Office
ATTN: DRXRO-PH (Dr. Lontz)
DRXRO-IP (In Turn)
PO Box 12211
001 Research Triangle Park, NC 27709

556 HQ, TCATA
Technical Information Center
ATTN: Mrs. Ruth Reynolds
001 Fort Hood, TX 76544

568 Commander
US Army Mobility Eqp Res & Dev Cmd
ATTN: DRDME-R
001 Fort Belvoir, VA 22060

604 Chief
Ofc of Missile Electronic Warfare
Electronic Warfare Lab, ERADCOM
001 White Sands Missile Range, NM 88002

606 Chief
Intel Materiel Dev & Support Ofc
Electronic Warfare Lab, ERADCOM
001 Fort Meade, MD 20755

608 Commander
ARRADCOM
DRDAR-TSB-S
001 Aberdeen Proving Ground, MD 21005

614 Cdr, ERADCOM
ATTN: DRDEL-LL, -SB, -AP (In Turn)
2800 Powder Mill Road
001 Adelphi, MD 27083

617 Cdr, ERADCOM
ATTN: DRDEL-AQ
2800 Powder Mill Road
001 Adelphi, MD 20783

619 Cdr, ERADCOM
ATTN: DRDEL-PA, -ILS, -ED (In Turn)
2800 Powder Mill Road
001 Adelphi, MD 20783

701 MTI — Lincoln Laboratory
ATTN: Library (RM A-082)
PO Box 73
002 Lexington, MA 02173

703 NASA Scientific & Tech Info Facility
Baltimore/Washington Intl Airport
001 PO Box 8757, MD 21240

704 National Bureau of Standards
Bldg 225, RM A-331
ATTN: Mr. Leedy
001 Washington, DC 20231

707 TACTEC
Batelle Memorial Institute
505 King Avenue
001 Columbus, OH 43201

ELECTRONICS TECHNOLOGY AND DEVICES LABORATORY
SUPPLEMENTAL CONTRACT DISTRIBUTION LIST (CONT)
(ELECTIVE)

Coordinated Science Laboratory
University of Illinois
Urbana, Illinois 61801
ATTN: Dr. Bill J. Hunsinger (1)

Dr. J.S. Bryant
OCRD
ATTN: DARD-ARP
Washington, DC 20310 (1)

Dr. R. LaRosa
Hazeltine Corporation
Greenlawn, New York 11740 (1)

General Electric Co.
Electronics Lab
Electronics Park
Syracuse, NY 13201
ATTN: Mr. S. Wanuga (1)

Air Force Cambridge Labs
ATTN: CRDR (Dr. P. Carr & Dr. A.J. Slobodnik)
Bedford, MA 01730 (2)

Mr. R. Weglein
Hughes Research Laboratories
3011 Malibu Canyon Road
Malibu, California 90265 (1)

Mr. H. Bush CORC
RADC
Griffiss Air Force Base
New York 13440 (1)

Dr. Tom Bristol
Hughes Aircraft Company
Ground Systems Group
Bldg 600/MS D235
1901 W. Malvern
Fullerton, CA 92634 (2)

Commander, AFAL
ATTN: Mr. W.J. Edwards, TEA
Wright-Patterson AFB, Ohio 45433 (1)

Anderson Laboratories, Inc.
1280 Blue Hills Ave
ATTN: Dr. A.A. Comparini
Bloomfield, Conn. 06002 (1)

Mr. Henry Friedman
RADC/OCTE
Griffiss AFB, NY 13440 (1)

Autonetics, Division of North American Rockwell
P.O. Box 4173
3370 Miraloma Avenue
Anaheim, CA 92802
ATTN: Dr. G.R. Pulliam (1)

General Dynamics, Electronics Division
P.O. Box 81127
San Diego, CA 92138
ATTN: Mr. R. Badewitz (1)

Texas Instruments, Inc.
P.O. Box 5936
13500 N. Central Expressway
Dallas, Texas 75222
ATTN: Dr. L.T. Clairborne (2)

Raytheon Company
Research Division
28 Seyon Street
Waltham, Massachusetts 02154
ATTN: Dr. M.B. Schulz (1)

Sperry Rand Research Center
100 North Road
Sudbury, Massachusetts 01776
ATTN: Dr. H. Van De Vaart (1)

Microwave Laboratory
W.W. Hansen Laboratories of Physics
Stanford University
Stanford, CA 94305
ATTN: Dr. H.J. Shaw (2)

ELECTRONICS TECHNOLOGY AND DEVICES LABORATORY
SUPPLEMENTAL CONTRACT DISTRIBUTION LIST (CONT)
(ELECTIVE)

Polytechnic Institute of Brooklyn
Route No. 110
Farmingdale, NY 11735
ATTN: Dr. A.A. Oliner (1)

Westinghouse Electric Corp.
Research & Development Center
Beulah Road
Pittsburgh, PA 15235
ATTN: Dr. J. DeKlerk (1)

Stanford Research Institute
Menlo Park, CA 94025
ATTN: Dr. A. Bahr (1)

International Business Machines Corp.
Research Division
P.O. Box 218
Yorktown Heights, NY 10598
ATTN: Dr. F. Bill (1)

TRW
Defense and Space Sys Group
One Space Park
Redondo Beach, CA 90278
ATTN: Dr. R.S. Kagiwada (1)

Tektronix Inc.
P.O. Box 500
Beaverton, OR 97077
ATTN: Dr. R. Li (1)

Dr. Fred S. Hickernell
Integrated Circuit Facility
Motorola Government Electronics Division
8201 East McDowell Road
Scottsdale, AZ 85257 (1)

Prof. H.F. Tiersten
Jonsson Engineering Center
Rensselaer Polytechnic Institute
Troy, NY 12181 (1)

McGill University
ATTN: G.W. Farnell
Montreal 110, Canada (1)

Advanced Technology Center, Inc.
Subsidiary of LTV Aerospace Corp.
P.O. Box 6144
Dallas, Texas 75222
ATTN: Mr. A.E. Sobey (1)

United Aircraft Research Labs
ATTN: Dr. Thomas W. Grudkowski
East Hartford, Conn. 06108 (1)

Science Center
Rockwell International
Thousand Oaks, CA 91360
ATTN: Dr. T.C. Lim (1)

University of Southern CA
Electronic Science Lab
School of Engineering
University Park, Los Angeles
California 900
ATTN: Dr. K. Lakin, SSC 303 (1)

SAWTEK, Inc.
P.O. Box 7756
2451 Shader Road
Orlando, Florida 32854
ATTN: Mr. S. Miller (1)

Prof. P.C.Y. Lee
School of Engineering
Princeton University
Princeton, NJ 08540 (1)

Mr. John A. Kusters
Hewlett-Packard
5301 Stevens Creek Boulevard
Santa Clara, CA 95050 (1)

Dr. Tom Young
Sandia Laboratories
P.O. Box 5800
Albuquerque, NM 87185 (1)

Dr. William J. Tanski
Sperry Research Center
100 North Road
Sudbury, MA 01776 (1)

ELECTRONICS TECHNOLOGY AND DEVICES LABORATORY
SUPPLEMENTAL CONTRACT DISTRIBUTION LIST (CONT)
(ELECTIVE)

Dr. B.A. Auld
E.L. Ginzton Laboratory
Stanford University
Stanford, CA 94305 (1)

Mr. Marvin E. Frerking
MS 137-138
Collins Radio Company
855 35th Street, NE
Cedar Rapids, IA 52406 (1)

Dr. William R. Shreve
HP Laboratories
1501 Page Mill Road
Palo Alto, CA 94304 (1)

Dr. Thomas M. Reeder
MS 50-362
Tektronix, Inc.
P.O. Box 500
Beaverton, OR 97077 (1)

Dr. Robert L. Rosenberg
Bell Laboratories
Crawfords Corner Road
Holmdel, NJ 07733 (1)

Dr. B.K. Sinha
Schlumberger-Doll Research Center
P.O. Box 307
Ridgefield, CT 06877 (1)

Dr. Robert S. Wagers
Texas Instruments, Inc.
13500 N. Central Expwy.
P.O. Box 225936, MS 134
Dallas, TX 75265 (1)

Dr. Richard C. Williamson
Lincoln Laboratory
P.O. Box 73
Lexington, MA 02173 (1)

SUPPLEMENT TO DISTRIBUTION LIST

D. Chrissotimos, Code 763
National Aeronautics and Space Administration
Goddard Space Flight Center
Greenbelt, MD 20771 (1)

Naval Research Laboratories
Code 5237
Washington, DC 20375
ATTN: Dr. D. Webb (1)

HQ ESD (DRI)
L.G. Hanscom AFB
Bedford, MA 01731 (1)

Commander
US Army Missile Command
ATTN: DRSMI-RE (Mr. Pittman)
Redstone Arsenal, AL 35809 (1)

Army Materials and Mechanics Research Center (AMMRC)
Watertown, MA 02172
ATTN: DMXMR-EO (1)

Commander, Picatinny Arsenal
ATTN: SARPA-FR-S
Bldg. 350
Dover, NJ 07801 (2)

A. Kahan
RADC/ESE
Hanscom AFB
Bedford, MA 01731 (1)

Dr. Robert O'Connell
Department of EE
Univ. of Missouri - Columbia
Columbia, MO 65201 (1)

Prof. John F. Vetelino
Dept of EE
Univ. of Maine - Orono
Orono, ME 04469 (1)

SUPPLEMENT TO DISTRIBUTION LIST

Dr. Robert O'Connell
Department of EE
University of Missouri - Columbia
Columbia, MO 65201 (1)

Prof. John F. Vetelino
Dept of EE
University of Maine - Orono
Orono, ME 04469 (1)

Dr. Franz Sauerland
Transat Corp.
3713 Lee Road
Shaker Heights, OH 44120 (1)

Mr. Leon Marchand
Damon Corp.
80 Wilson Way
Westwood, MA 02090 (1)


DAT
FILM